Structural Engineering and Mechanics, Vol. 15, No. 6 (2003) 717-733
DOI: http://dx.doi.org/10.12989/sem.2003.15.6.717

Time domain earthquake response analysis method for 2-D soil-structure interaction systems

Doo Kie Kim†

Department of Civil Engineering, Kunsan National University, San 68, Miryong-Dong, Kunsan, Jeonbuk 573-701, Korea

Chung-Bang Yun‡

Department of Civil Engineering, Korea Advanced Institute of Science and Technology, 373-1, Kusong-Dong, Yusong-Ku, Daejeon 305-701, Korea

(Received July 29, 2002, Accepted March 19, 2003)

Abstract. A time domain method is presented for soil-structure interaction analysis under seismic excitations. It is based on the finite element formulation incorporating infinite elements for the far field soil region. Equivalent earthquake input forces are calculated based on the free field responses along the interface between the near and far field soil regions utilizing the fixed exterior boundary method in the frequency domain. Then, the input forces are transformed into the time domain by using inverse Fourier transform. The dynamic stiffness matrices of the far field soil region formulated using the analytical frequency-dependent infinite elements in the frequency domain can be easily transformed into the corresponding matrices in the time domain. Hence, the response can be analytically computed in the time domain. A recursive procedure is proposed to compute the interaction forces along the interface and the responses of the soil-structure system in the time domain. Earthquake response analyses have been carried out on a multi-layered half-space and a tunnel embedded in a layered half-space with the assumption of the linearity of the near and far field soil region, and results are compared with those obtained by the conventional method in the frequency domain.

Key words: soil-structure interaction; analytical frequency-dependent infinite element; earthquake response analysis; time domain analysis; recursive procedure.

1. Introduction

The earthquake responses of massive civil engineering structures may be influenced by the soil-structure interaction as well as the dynamic characteristics of the excitations and the structures. The effect of the soil-structure interaction is noticeable especially for stiff and massive structures resting on the relatively soft ground. It may cause the dynamic characteristics of the structural response altered significantly. Thus the interaction effects have to be considered in the dynamic analysis of the structures in a semi-infinite soil medium (Wolf 1985, Betti *et al*. 1993).

† Assistant Professor
‡ Professor

Two important things that may distinguish the soil-structure interaction system from the general structural dynamic system are the unbounded nature and the nonlinear characteristics of the soil medium. In general, the radiational damping in an unbounded soil medium can be described more easily in the frequency domain than in the time domain, since it is dependent on the excitation frequencies (Wolf 1985). On the other hand, the nonlinear behavior of the soil medium can be considered more easily in the time domain (Wolf 1988, Wolf and Song 1996). Thus supplementary treatments of soil-structure interaction in the frequency and time domains may be needed to consider both characteristics of the soil medium. At present, most of the well-known computer programs for soil-structure interaction analysis are based on the frequency domain analysis incorporating the equivalent linearization technique to consider the nonlinearity of the soil medium (Seed and Idriss 1970, Kramer 1996, Lysmer *et al*. 1975, ASD International 1985, Lysmer *et al*. 1988, Tzong and Penzien 1983).

In recent years, several time domain methods have been proposed to study nonlinear behaviors of the soil medium, effects of pore water, and nonlinear conditions along the interface between soil and structure. One method is the coupling of the boundary and the finite element methods (Karabalis adn Beskos 1985, Estorff 1991, Guan and Novak 1994). In this method the structure and the near field soil region are modeled using finite elements, while the far field soil region is represented using boundary elements. However, it has been generally difficult to derive fundamental solutions in layered soils and to couple the boundary elements with the finite elements. In recent researches, significant advance in the time domain has been made in this area (Song and Wolf 1999, Zhang *et al.* 1999). This method, which does not require fundamental solution, has been successfully used in coupling with finite elements and applied for three dimensional soil-structure interactions in the time domain. Another method is the one using the transformation of the dynamic stiffness matrix into the terms in the time domain (Hayashi and Katukura 1990). However, the dynamic stiffness matrix for the far field region is usually obtained numerically at each frequency. Therefore, the transformation has to be carried out numerically using discrete Fourier transform or discrete z-transform, which requires tremendous computational time and huge computer-memory for realistic problems.

This paper presents a time domain method for soil-structure interaction analysis under seismic loadings. It is based on the finite element formulation incorporating analytical frequency-dependent infinite elements for the far field soil region (Yun *et al.* 2000, Kim and Yun 2000). The equivalent earthquake input forces are calculated based on the free field responses (Wolf and Obernhuber 1982) along the interface between the near and far field soil regions using the fixed exterior boundary method (Zhao and Valliappan 1993). The earthquake input forces are computed in the frequency domain, then converted into the time domain. The interaction forces along the interface during the earthquake response analysis are computed using a recursive procedure developed in this study. For verification, earthquake response analysis has been carried out for a multi-layered half-space with the assumption of the linearity of the near- and far field soil region, and the results are compared with the free field responses obtained by the conventional frequency domain method (Wolf and Obernhuber 1982, Zhao and Valliappan 1993, Zhang and Zhao 1988). Earthquake response analysis has been also performed for a tunnel embedded in a layered half-space to show the applicability of the proposed method in the field.

2. Modeling of far field soil region

The structure and the near field soil region are modeled using 9-node plane strain finite elements, and the far field soil region is represented using horizontal, vertical and left and right corner infinite elements (Yun *et al.* 2000); i.e., HIE, VIE, LCIE, and RCIE as shown in Fig. 1. Horizontal and vertical infinite elements have 3 nodes, and right and left corner infinite elements have 1 node on the interface between the near and the far field soil regions, and example shape functions for analytical frequency-dependent infinite elements are shown in Fig. 2.

Referring to Fig. 1(b), the mapping from the local coordinates (ξ, η) to the global coordinates (x, z) is defined for three kinds of infinite elements as

$$x = x_0(1+\xi), \quad z = \sum_{j=1}^{N} L_j(\eta) z_j \quad \text{for HIE } ((x,z) \in \Omega_H^e) \tag{1}$$

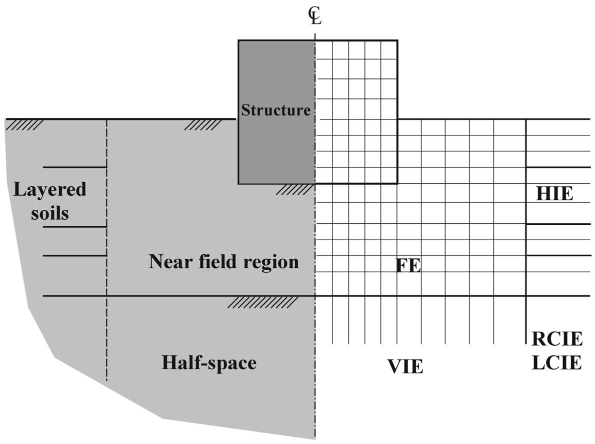

(a) Analysis model

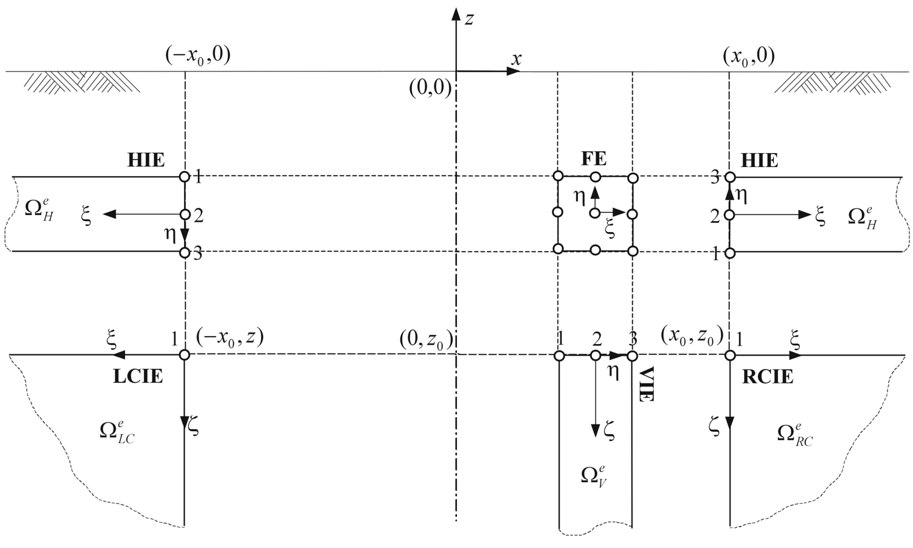

(b) Global and local coordinates

Fig. 1 Soil-structure interaction system in 2-dimensional soil medium

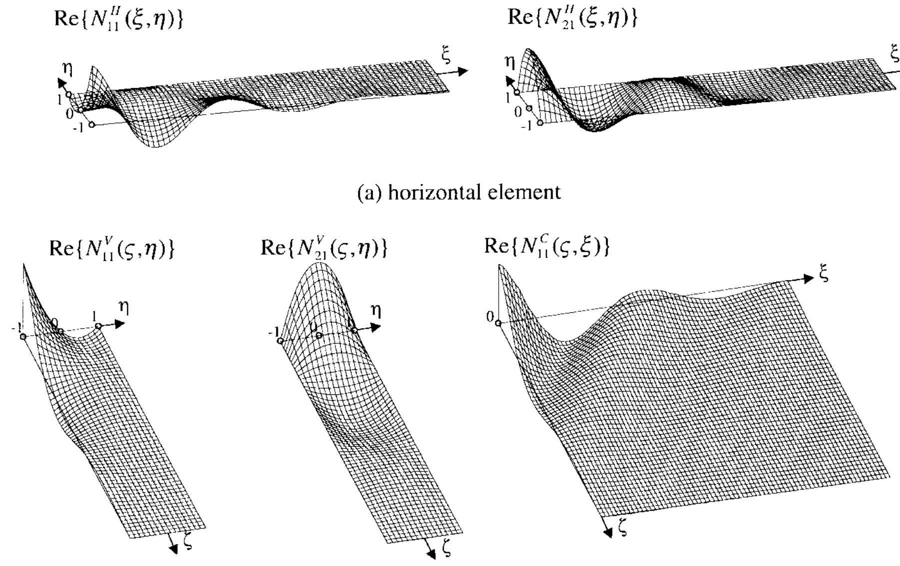

(a) horizontal element

(b) verticale element

(c) corner element

Fig. 2 Real parts of typical shape functions for analytical frequency dependent infinite elements

$$x = x_0(1+\xi), \quad z = z_0(1-\zeta) \quad \text{for LCIE or RCIE } ((x,z) \in \Omega_{LC}^{e} \quad \text{or} \quad \Omega_{RC}^{e}) \tag{2}$$

$$x = \sum_{j=1}^{N} L_j(\eta)x_j, \quad z = z_0(1-\zeta) \quad \text{for VIE } ((x,z) \in \Omega_{V}^{e}) \tag{3}$$

where x_j and z_j are the global coordinates at node j; x_0 and z_0 are the global coordinates of the corner point in the region Ω_{LC} or Ω_{RC}; N is the number of nodes for horizontal and vertical infinite elements; and $L_j(\eta)$ is the Lagrange polynomial which has unit value at the j-th node while zero at other nodes. The ranges of the local coordinates are: $\eta \in [-1, 1]$, $\xi \in [0, \infty]$ and $\zeta \in [0, \infty]$.

For the purpose of the time domain analysis in this study, the shape functions for each infinite element are approximately taken as those of the analytical frequency dependent infinite elements (Yun *et al.* 2000) as

$$N_{jm}^{H}(\xi, \eta; \omega) = L_j(\eta) f_m(\xi; \omega) \quad \text{for HIE} \tag{4}$$

$$N_{mp}^{C}(\zeta, \xi; \omega) = f_m(\xi; \omega) g_p(\zeta; \omega) \quad \text{for LCIE and RCIE} \tag{5}$$

$$N_{jp}^{V}(\zeta, \eta; \omega) = L_j(\eta) g_p(\zeta; \omega) \quad \text{for VIE} \tag{6}$$

where $f_m(\xi;\omega)$ and $g_p(\zeta;\omega)$ are horizontal and vertical wave functions derived from the approximate expressions for the propagating waves in layered elastic media as (Yun *et al.* 2000)

$$f_m(\xi;\omega) = e^{-C_m(\omega)x_0\xi}, \qquad g_p(\zeta;\omega) = e^{-C_p(\omega)z_0\zeta} \tag{7}$$

where

$$C_m(\omega) = (a + i\omega)\begin{Bmatrix} \frac{1}{c_s} \\ \frac{1}{c_p} \\ \frac{1}{\bar{c}_{rl}} \end{Bmatrix}, \qquad C_p(\omega) = (a + i\omega)\begin{Bmatrix} \frac{1}{c_s} \\ \frac{1}{c_p} \end{Bmatrix} \tag{8}$$

where c_s, c_p, and $\bar{c}_{rl}$ are wave velocities for S-wave, P-wave and the mean value of the l-th Rayleigh wave ($l = 1, ..., N_r$) in the frequency range of concern; and N_r is the number of Rayleigh waves employed in the displacement approximation. The positive constant, a, in Eq. (8) is related to the geometric attenuation, and taken to be the same for all wave components. Validity of the approximation in Eqs. (7) and (8) was extensively discussed in Yun *et al.* (2000).

The mass and stiffness component matrices of the infinite element associated with the j-th and the k-th shape functions are defined as

$$\boldsymbol{m}_{jk} = \rho\int_{\Omega} N_j^T N_k d\Omega \boldsymbol{I} \tag{9}$$

$$\boldsymbol{k}_{jk} = \int_{\Omega} \boldsymbol{B}_j^T \boldsymbol{D} \boldsymbol{B}_k d\Omega \tag{10}$$

where ρ is the mass density; $\boldsymbol{I}$ and $\boldsymbol{D}$ are the (2 × 2) identity and the elasticity matrices; and $\boldsymbol{B}_j$ and $\boldsymbol{B}_k$ are the strain-displacement matrices associated with shape function N_j and N_k, respectively.

Employing the shape functions with the wave functions described in Eqs. (7) and (8), the mass and stiffness matrices for each infinite element can be obtained in analytical forms of the exciting frequency and constant matrices as (Yun *et al.* 2000)

$$\boldsymbol{M}^{(e)}(\omega) = \frac{1}{a + i\omega}\boldsymbol{M}_0^{(e)} + \frac{1}{(a + i\omega)^2}\boldsymbol{M}_1^{(e)} \tag{11}$$

$$\boldsymbol{K}^{(e)}(\omega) = \boldsymbol{K}_0^{(e)} + (a + i\omega)\boldsymbol{K}_1^{(e)} + \frac{1}{a + i\omega}\boldsymbol{K}_2^{(e)} \tag{12}$$

where $\boldsymbol{M}_0^{(e)}, \boldsymbol{M}_1^{(e)}, \boldsymbol{K}_0^{(e)}, \boldsymbol{K}_1^{(e)}$ and $\boldsymbol{K}_2^{(e)}$ are real-valued constant matrices if the material damping in the far field soil is ignored, which is generally much smaller than the radiation damping.

Assembling the mass and stiffness matrices of the analytical frequency-dependent infinite elements, the dynamic stiffness matrix of the far field soil region, $\boldsymbol{S}_{ee}^F(\omega)$, can be obtained as (Yun *et al.* 2000)

$$\boldsymbol{S}_{ee}^F(\omega) = \boldsymbol{S}_0^F + i\omega\boldsymbol{S}_1^F + \frac{1}{a + i\omega}\boldsymbol{S}_2^F + \frac{1}{(a + i\omega)^2}\boldsymbol{S}_3^F \tag{13}$$

where $\boldsymbol{S}_0^F, \boldsymbol{S}_1^F, \boldsymbol{S}_2^F$, and $\boldsymbol{S}_3^F$ are real-valued constant matrices if the material damping in the far field soil is ignored :

$$\boldsymbol{S}_0^F = \boldsymbol{K}_0^F + a\boldsymbol{K}_1^F - a\boldsymbol{M}_0^F + \boldsymbol{M}_1^F \tag{14a}$$

$$S_1^F = K_1^F + M_0^F \tag{14b}$$

$$S_2^F = K_2^F + a^2 M_0^F - 2aM_1^F \tag{14c}$$

$$S_3^F = a^2 M_1^F \tag{14d}$$

in which $\boldsymbol{M}_0^F, \boldsymbol{M}_1^F, \boldsymbol{K}_0^F, \boldsymbol{K}_1^F$ and $\boldsymbol{K}_2^F$ are the assemblages of the element-level matrices $\boldsymbol{M}_0^{(e)}, \boldsymbol{M}_1^{(e)}$ $\boldsymbol{K}_0^{(e)}, \boldsymbol{K}_1^{(e)}$ and $\boldsymbol{K}_2^{(e)}$ respectively.

3. Earthquake response analysis in time domain

At first, the equivalent earthquake input force $\boldsymbol{f}_e^f$ is evaluated along Γ_e from the free field responses using the rigid exterior boundary method (Zhao and Valliappan 1993, Zhang and Zhao 1988) as shown in Fig. 3. Earthquake inputs are regarded as traveling P- and SV-waves that are incident vertically to the near field soil region.

$$\boldsymbol{f}_e^f(\omega) = \boldsymbol{S}_{ee}^F(\omega)\boldsymbol{u}_e^f(\omega) - \boldsymbol{A}\boldsymbol{t}_e^f(\omega) \tag{15}$$

where $\boldsymbol{u}_e^f$ and $\boldsymbol{t}_e^f$ are the displacement and the traction along Γ_e for the free field soil medium subjected to the earthquake excitation; and $\boldsymbol{A}$ is the matrix to transform the traction into the force.

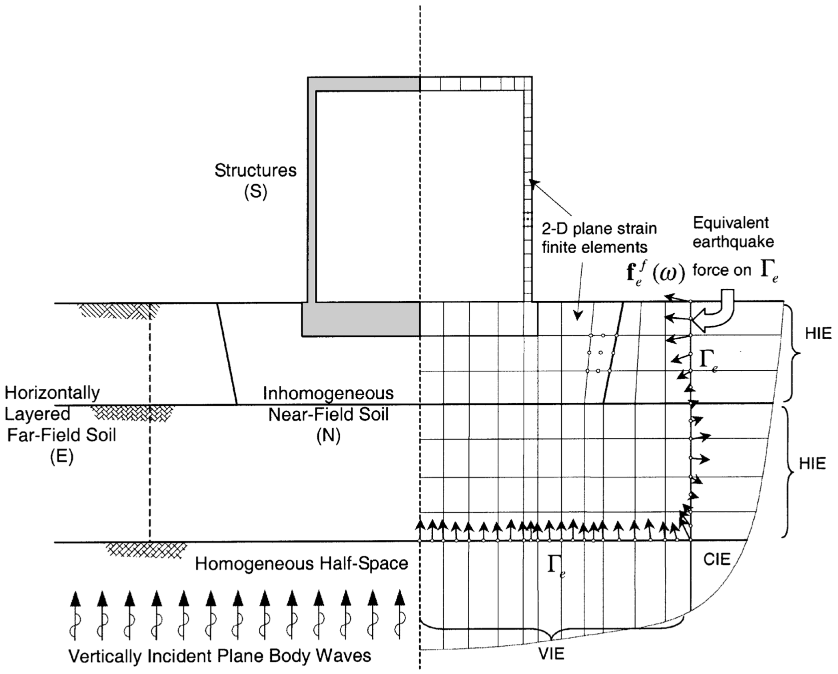

Fig. 3 Concept of the proposed earthquake response analysis

Then, the equation of motion for the soil-structure interaction system subjected to $\boldsymbol{f}_e^f(\omega)$ can be written in the frequency domain as (Wolf 1985)

$$\begin{bmatrix} \boldsymbol{S}_{nn}(\omega) & \boldsymbol{S}_{ne}(\omega) \\ \boldsymbol{S}_{en}(\omega) & \boldsymbol{S}_{ee}(\omega) + \boldsymbol{S}_{ee}^F(\omega) \end{bmatrix} \begin{Bmatrix} \boldsymbol{u}_n(\omega) \\ \boldsymbol{u}_e(\omega) \end{Bmatrix} = \begin{Bmatrix} \boldsymbol{0} \\ \boldsymbol{f}_e^f(\omega) \end{Bmatrix} \tag{16}$$

where subscript n stands for the degrees-of-freedom (DOF's) of the structure and the near field soil region, while e denotes those on the interface Γ_e. For the computational convenience, Eq. (16) can be rewritten as

$$\begin{bmatrix} \boldsymbol{S}_{nn}(\omega) & \boldsymbol{S}_{ne}(\omega) \\ \boldsymbol{S}_{en}(\omega) & \boldsymbol{S}_{ee}(\omega) \end{bmatrix} \begin{Bmatrix} \boldsymbol{u}_n(\omega) \\ \boldsymbol{u}_e(\omega) \end{Bmatrix} = \begin{Bmatrix} \boldsymbol{0} \\ \boldsymbol{f}_e^f(\omega) + \boldsymbol{f}_e(\omega) \end{Bmatrix} \tag{17}$$

$$\boldsymbol{f}_e(\omega) = -\boldsymbol{S}_{ee}^F(\omega)\boldsymbol{u}_e(\omega) \tag{18}$$

where $\boldsymbol{f}_e(\omega)$ may be defined as the interaction force which depends on the response of the interface Γ_e with the far field soil region.

For time domain analysis, the interaction force $\boldsymbol{f}_e(\omega)$ can be transformed as (Wolf 1988, Wolf and Song 1996)

$$\boldsymbol{f}_e(t) = -\int_0^t \boldsymbol{S}_{ee}^F(t-\tau)\boldsymbol{u}_e(\tau)d\tau \tag{19}$$

where $\boldsymbol{S}_{ee}^F(t)$ is the inverse Fourier transform of $\boldsymbol{S}_{ee}^F(\omega)$, which can be obtained from Eq. (13) in an analytical form as (Kim and Yun 2000)

$$\boldsymbol{S}_{ee}^F(t) = \boldsymbol{F}^{-1}\{\boldsymbol{S}_{ee}^F(\omega)\} = \frac{1}{2\pi}\int_{-\infty}^{+\infty} \boldsymbol{S}_{ee}^F(\omega)e^{i\omega t}d\omega \tag{20}$$

$$\boldsymbol{S}_{ee}^F(t) = \boldsymbol{S}_0^F\delta(t) + \boldsymbol{S}_1^F\dot{\delta}(t) + \boldsymbol{S}_2^F e^{-at}H(t) + \boldsymbol{S}_3^F t e^{-at}H(t) \tag{21}$$

where $H(t)$ is unit step function; and $\delta(t)$ and $\dot{\delta}(t)$ are Dirac-delta function and its derivative respectively. From Eqs. (19) and (21), the interaction force can be also obtained analytically as (Kim and Yun 2000)

$$\boldsymbol{f}_e(t) = -\boldsymbol{S}_0^F\boldsymbol{u}_e(t) - \boldsymbol{S}_1^F\dot{\boldsymbol{u}}_e(t) - \int_0^t \{\boldsymbol{S}_2^F + (t-\tau)\boldsymbol{S}_3^F\}e^{-a(t-\tau)}\boldsymbol{u}_e(\tau)d\tau \tag{22}$$

Finally, the time domain equation of motion for the soil-structure interaction system can be derived from Eqs. (17) and (22) as

$$\begin{bmatrix} \boldsymbol{M}_{nn} & \boldsymbol{M}_{ne} \\ \boldsymbol{M}_{en} & \boldsymbol{M}_{ee} \end{bmatrix} \begin{Bmatrix} \ddot{\boldsymbol{u}}_n(t) \\ \ddot{\boldsymbol{u}}_e(t) \end{Bmatrix} + \begin{bmatrix} \boldsymbol{0} & \boldsymbol{0} \\ \boldsymbol{0} & \boldsymbol{S}_1^F \end{bmatrix} \begin{Bmatrix} \dot{\boldsymbol{u}}_n(t) \\ \dot{\boldsymbol{u}}_e(t) \end{Bmatrix} + \begin{bmatrix} \boldsymbol{K}_{nn} & \boldsymbol{K}_{ne} \\ \boldsymbol{K}_{en} & \boldsymbol{K}_{ee} + \boldsymbol{S}_0^F \end{bmatrix} \begin{Bmatrix} \boldsymbol{u}_n(t) \\ \boldsymbol{u}_e(t) \end{Bmatrix} = \begin{Bmatrix} \boldsymbol{0} \\ \boldsymbol{f}_e^f(t) + \bar{\boldsymbol{f}}_e(t) \end{Bmatrix} \tag{23}$$

where $\boldsymbol{M}_{nn}$, $\boldsymbol{M}_{ne}$, $\boldsymbol{M}_{en}$, $\boldsymbol{M}_{ee}$, $\boldsymbol{K}_{nn}$, $\boldsymbol{K}_{ne}$, $\boldsymbol{K}_{en}$, and $\boldsymbol{K}_{ee}$ are the conventional mass and stiffness matrices for the structure and the near field soil; $\boldsymbol{f}_e^f(t)$ is the equivalent earthquake input force along Γ_e obtained from inverse Fourier Transform of $\boldsymbol{f}_e^f(\omega)$; and $\bar{\boldsymbol{f}}_e(t)$ is the third term of the interaction force $\boldsymbol{f}_e(t)$ in Eq. (22) as

$$\bar{\boldsymbol{f}}_e(t) = -\int_0^t \{\boldsymbol{S}_2^F + (t-\tau)\boldsymbol{S}_3^F\} e^{-a(t-\tau)} \boldsymbol{u}_e(\tau) d\tau \tag{24}$$

In Eq. (23), a nonlinear restoring force and linear damping in the near field as well as $\boldsymbol{f}_e^f(\omega)$ and $\bar{\boldsymbol{f}}_e(t)$ can be included for more practical and robust application of the proposed method. However, only the linear radiational damping of the soil region in the present paper is considered.

4. Recursive procedure for response in time domain

The present recursive procedure in the time domain is basically using the Newmark-Beta method although approximations at various stages are being made.

The new interaction force $\bar{\boldsymbol{f}}_e(t)$ in Eq. (24) can be decomposed as

$$\bar{\boldsymbol{f}}_e(t) = \bar{\boldsymbol{f}}_{e1}(t) + \bar{\boldsymbol{f}}_{e2}(t) + \Delta\bar{\boldsymbol{f}}_e(t) \tag{25}$$

where

$$\bar{\boldsymbol{f}}_{e1}(t) = -\int_0^{t-\Delta t} \boldsymbol{S}_2^F e^{-a(t-\tau)} \boldsymbol{u}_e(\tau) d\tau \tag{26a}$$

$$\bar{\boldsymbol{f}}_{e2}(t) = -\int_0^{t-\Delta t} (t-\tau)\boldsymbol{S}_3^F e^{-a(t-\tau)} \boldsymbol{u}_e(\tau) d\tau \tag{26b}$$

and

$$\Delta\bar{\boldsymbol{f}}_e(t) = -\int_{t-\Delta t}^{t} \{\boldsymbol{S}_2^F + (t-\tau)\boldsymbol{S}_3^F\} e^{-a(t-\tau)} \boldsymbol{u}_e(\tau) d\tau \tag{26c}$$

Numerical evaluation of the convolution integrals in Eqs. (26a)-(26c) would be very time consuming. Therefore an efficient recursive procedure is developed, assuming a linear variation of the responses between two adjacent times. The Eqs. (26a)-(26c) can be approximately rewritten into discrete time forms at $t = n\Delta t$ as

$$\begin{aligned} \bar{\boldsymbol{f}}_{e1}(t) = {} & e^{-a\Delta t} \bar{\boldsymbol{f}}_{e1}(t-\Delta t) - \boldsymbol{S}_2^F \frac{e^{-2a\Delta t}}{a^2 \Delta t} [\{1 - e^{a\Delta t}(1 - a\Delta t)\} \boldsymbol{u}_e(t-\Delta t) \\ & - \{1 + a\Delta t - e^{a\Delta t}\} \boldsymbol{u}_e(t-2\Delta t)] \end{aligned} \tag{27a}$$

$$\begin{aligned} \bar{\boldsymbol{f}}_{e2}(t) = {} & 2e^{-a\Delta t} \bar{\boldsymbol{f}}_{e2}(t-\Delta t) - e^{-2a\Delta t} \bar{\boldsymbol{f}}_{e2}(t-2\Delta t) \\ & + \boldsymbol{S}_3^F \frac{1}{a^3 \Delta t} [e^{-2a\Delta t}\{-2 - 2a\Delta t + e^{a\Delta t}(2 - a^2(\Delta t)^2)\} \boldsymbol{u}_e(t-\Delta t) \\ & + e^{-3a\Delta t}\{2 + a\Delta t + e^{a\Delta t}(4a\Delta t + 2a^2(\Delta t)^2) - 2^{2a\Delta t}(2 + a\Delta t)\} \boldsymbol{u}_e(t-2\Delta t) \\ & + e^{-3a\Delta t}\{-2 - 2a\Delta t - a^2(\Delta t^2) + 2e^{a\Delta t}\} \boldsymbol{u}_e(t-3\Delta t)] \end{aligned} \tag{27b}$$

$$\Delta\bar{\boldsymbol{f}}_e(t) = -\boldsymbol{S}_2^F\frac{1}{a^2\Delta t}[\{-1 + a\Delta t + e^{-a\Delta t}\}\boldsymbol{u}_e(t) + \{1 - e^{-a\Delta t}(1 + a\Delta t)\}\boldsymbol{u}_e(t-\Delta t)]$$
$$-\boldsymbol{S}_3^F\frac{1}{a^3\Delta t}[\{-2 + a\Delta t + e^{-a\Delta t}(2 + a\Delta t)\}\boldsymbol{u}_e(t)$$
$$+\{2 - e^{-a\Delta t}(2 + 2a\Delta t + a^2(\Delta t)^2)\}\boldsymbol{u}_e(t-\Delta t)] \tag{27c}$$

Incorporating the above equations, the Eq. (23) can be approximately rewritten into discrete time forms at $t = n\Delta t$ as

$$\begin{bmatrix}\boldsymbol{M}_{nn} & \boldsymbol{M}_{ne}\\ \boldsymbol{M}_{ns} & \boldsymbol{M}_{ee}\end{bmatrix}\begin{Bmatrix}\ddot{\boldsymbol{u}}_n(t)\\ \ddot{\boldsymbol{u}}_e(t)\end{Bmatrix} + \begin{bmatrix}\boldsymbol{0} & \boldsymbol{0}\\ \boldsymbol{0} & \boldsymbol{S}_1^F\end{bmatrix}\begin{Bmatrix}\dot{\boldsymbol{u}}_n(t)\\ \dot{\boldsymbol{u}}_e(t)\end{Bmatrix} + \begin{bmatrix}\boldsymbol{K}_{nn} & \boldsymbol{K}_{ne}\\ \boldsymbol{K}_{en} & \boldsymbol{K}_{ee} + \boldsymbol{S}_0^F + \alpha_2\boldsymbol{S}_2^F + \alpha_3\boldsymbol{S}_3^F\end{bmatrix}\begin{Bmatrix}\boldsymbol{u}_n(t)\\ \boldsymbol{u}_e(t)\end{Bmatrix}$$
$$= \begin{Bmatrix}0\\ \boldsymbol{f}_e^f(t) + \bar{\boldsymbol{f}}_{e1}(t) + \bar{\boldsymbol{f}}_{e2}(t) + (\beta_2\boldsymbol{S}_2^F + \beta_3\boldsymbol{S}_3^F)\boldsymbol{u}_e(t-\Delta t)\end{Bmatrix} \tag{28}$$

where α_2, α_3, β_2 and β_3 are real constants, which depend on a and Δt, as

$$\alpha_2 = \frac{1}{a^2\Delta t}\{-1 + a\Delta t + e^{-a\Delta t}\} \tag{29a}$$

$$\alpha_3 = \frac{1}{a^3\Delta t}\{-2 + a\Delta t + e^{-a\Delta t}(2 + a\Delta t)\} \tag{29b}$$

$$\beta_2 = \frac{1}{a^2\Delta t}\{-1 + e^{-a\Delta t}(1 + a\Delta t)\} \tag{29c}$$

$$\beta_3 = \frac{1}{a^2\Delta t}\{-2 + e^{-a\Delta t}(2 + 2a\Delta t + a^2(\Delta t)^2)\} \tag{29d}$$

In the present study, it is noteworthy that the convolution integrals for $\bar{\boldsymbol{f}}_{e1}(t)$ and $\bar{\boldsymbol{f}}_{e2}(t)$ are evaluated recursively as finite sums of a few past terms of $\bar{\boldsymbol{f}}_{e1}(t)$, $\bar{\boldsymbol{f}}_{e2}(t)$, and $\boldsymbol{u}_e(t)$. The recursive procedure for the numerical evaluation of the convolution integral in Eq. (28) is summarized in Table 1. In fact a similar procedure was proposed assuming a constant value of the response $\boldsymbol{u}_e(t)$ between two adjacent times by the present authors (Kim and Yun 2000). Hence the present formulation based on the linear variation may be considered as an improved one. The present time domain formulation based on the analytical frequency-dependent infinite elements is very straightforward and computationally very efficient in comparison with the methods using numerical transforms such as discrete Fourier transform or discrete *z*-transform, which usually require huge computational efforts (Wolf 1988, Wolf and Song 1996, Tzong and Penzien 1985).

5. Numerical examples

5.1 Free field responses of a layered soil medium

For verification of the proposed analysis procedure, earthquake response analysis of a multi-layered free field half-space shown in Fig. 4 is carried out. The near field soil region is discretized

Table 1 Recursive integration procedure

A. Initial Calculations:

1. Form, $\begin{bmatrix} \boldsymbol{M}_{nn} & \boldsymbol{M}_{ne} \\ \boldsymbol{M}_{en} & \boldsymbol{M}_{ee} \end{bmatrix}, \begin{bmatrix} \boldsymbol{0} & \boldsymbol{0} \\ \boldsymbol{0} & \boldsymbol{S}_1^F \end{bmatrix}, \begin{bmatrix} \boldsymbol{K}_{nn} & \boldsymbol{K}_{ne} \\ \boldsymbol{K}_{en} & \boldsymbol{K}_{ee} + \boldsymbol{S}_0^F + \alpha_2 \boldsymbol{S}_2^F + \alpha_3 \boldsymbol{S}_3^F \end{bmatrix}$
2. Initialize accelerations $(\ddot{\boldsymbol{U}}(0))$, velocities $(\dot{\boldsymbol{U}}(0))$, and displacements $(\boldsymbol{U}(0))$;

$$\begin{Bmatrix} \ddot{\boldsymbol{u}}_n(\boldsymbol{0}) \\ \ddot{\boldsymbol{u}}_e(\boldsymbol{0}) \end{Bmatrix}, \begin{Bmatrix} \dot{\boldsymbol{u}}_n(\boldsymbol{0}) \\ \dot{\boldsymbol{u}}_e(\boldsymbol{0}) \end{Bmatrix}, \begin{Bmatrix} \boldsymbol{u}_n(\boldsymbol{0}) \\ \boldsymbol{u}_e(\boldsymbol{0}) \end{Bmatrix}$$

3. Set parameters;

$$\Delta t, \quad \gamma = \frac{1}{2}, \quad \beta = \frac{1}{4}$$

$$a_0 = \frac{1}{\beta(\Delta t)^2}, \quad a_1 = \frac{\gamma}{\beta \Delta t}, \quad a_2 = \frac{1}{\beta \Delta t}, \quad a_3 = \frac{1}{2\beta} - 1,$$

$$a_4 = \frac{\gamma}{\beta} - 1, \quad a_5 = \frac{\Delta t}{2}\left(\frac{\gamma}{\beta} - 2\right), \quad a_6 = \Delta t(1-\gamma), \quad a_7 = \gamma \Delta t$$

4. Form the effective stiffness matrix $\tilde{\boldsymbol{K}}$;

$$\tilde{\boldsymbol{K}} = \begin{bmatrix} \boldsymbol{K}_{nn} & \boldsymbol{K}_{ne} \\ \boldsymbol{K}_{en} & \boldsymbol{K}_{ee} + \boldsymbol{S}_0^F + \alpha_2 \boldsymbol{S}_2^F + \alpha_3 \boldsymbol{S}_3^F \end{bmatrix} + a_0 \begin{bmatrix} \boldsymbol{M}_{nn} & \boldsymbol{M}_{ne} \\ \boldsymbol{M}_{en} & \boldsymbol{M}_{ee} \end{bmatrix} + a_1 \begin{bmatrix} \boldsymbol{0} & \boldsymbol{0} \\ \boldsymbol{0} & \boldsymbol{S}_1^F \end{bmatrix}$$

B. For each time step:

1. Calculate $\boldsymbol{R}(t+\Delta t)$ at $(t+\Delta t)$;

$$\boldsymbol{R}(t+\Delta t) = \begin{Bmatrix} \boldsymbol{f}_n(t+\Delta t) \\ \bar{\boldsymbol{f}}_{e1}(t) + \bar{\boldsymbol{f}}_{e2}(t) + (\beta_2 \boldsymbol{S}_2^F + \beta_3 \boldsymbol{S}_3^F)\boldsymbol{u}_e(t-\Delta t) \end{Bmatrix}$$
$$+ \begin{bmatrix} \boldsymbol{M}_{nn} & \boldsymbol{M}_{ne} \\ \boldsymbol{M}_{en} & \boldsymbol{M}_{ee} \end{bmatrix}\left(a_0 \begin{Bmatrix} \boldsymbol{u}_n(t) \\ \boldsymbol{u}_e(t) \end{Bmatrix} + a_2 \begin{Bmatrix} \dot{\boldsymbol{u}}_n(t) \\ \dot{\boldsymbol{u}}_e(t) \end{Bmatrix} + a_3 \begin{Bmatrix} \ddot{\boldsymbol{u}}_n(t) \\ \ddot{\boldsymbol{u}}_e(t) \end{Bmatrix} \right)$$
$$+ \begin{bmatrix} \boldsymbol{0} & \boldsymbol{0} \\ \boldsymbol{0} & \boldsymbol{S}_1^F \end{bmatrix}\left(a_1 \begin{Bmatrix} \boldsymbol{u}_n(t) \\ \boldsymbol{u}_e(t) \end{Bmatrix} + a_4 \begin{Bmatrix} \dot{\boldsymbol{u}}_n(t) \\ \dot{\boldsymbol{u}}_e(t) \end{Bmatrix} + a_5 \begin{Bmatrix} \ddot{\boldsymbol{u}}_n(t) \\ \ddot{\boldsymbol{u}}_e(t) \end{Bmatrix} \right)$$

2. Solve $\boldsymbol{U}(t+\Delta t)$ at $(t+\Delta t)$;

$$\tilde{\boldsymbol{K}} \begin{Bmatrix} \boldsymbol{u}_n(t+\Delta t) \\ \boldsymbol{u}_e(t+\Delta t) \end{Bmatrix} = \boldsymbol{R}(t+\Delta t)$$

3. Calculate $\ddot{\boldsymbol{U}}(t+\Delta t)$, $\dot{\boldsymbol{U}}(t+\Delta t)$;

$$\begin{Bmatrix} \ddot{\boldsymbol{u}}_n(t+\Delta t) \\ \ddot{\boldsymbol{u}}_e(t+\Delta t) \end{Bmatrix} = a_0\left(\begin{Bmatrix} \boldsymbol{u}_n(t+\Delta t) \\ \boldsymbol{u}_e(t+\Delta t) \end{Bmatrix} - \begin{Bmatrix} \boldsymbol{u}_n(t) \\ \boldsymbol{u}_e(t) \end{Bmatrix} \right) - a_2 \begin{Bmatrix} \dot{\boldsymbol{u}}_n(t) \\ \dot{\boldsymbol{u}}_e(t) \end{Bmatrix} - a_3 \begin{Bmatrix} \ddot{\boldsymbol{u}}_n(t) \\ \ddot{\boldsymbol{u}}_e(t) \end{Bmatrix}$$
$$\begin{Bmatrix} \dot{\boldsymbol{u}}_n(t+\Delta t) \\ \dot{\boldsymbol{u}}_e(t+\Delta t) \end{Bmatrix} = \begin{Bmatrix} \dot{\boldsymbol{u}}_n(t) \\ \dot{\boldsymbol{u}}_e(t) \end{Bmatrix} + a_6 \begin{Bmatrix} \ddot{\boldsymbol{u}}_n(t) \\ \ddot{\boldsymbol{u}}_e(t) \end{Bmatrix} + a_7 \begin{Bmatrix} \ddot{\boldsymbol{u}}_n(t+\Delta t) \\ \ddot{\boldsymbol{u}}_e(t+\Delta t) \end{Bmatrix}$$

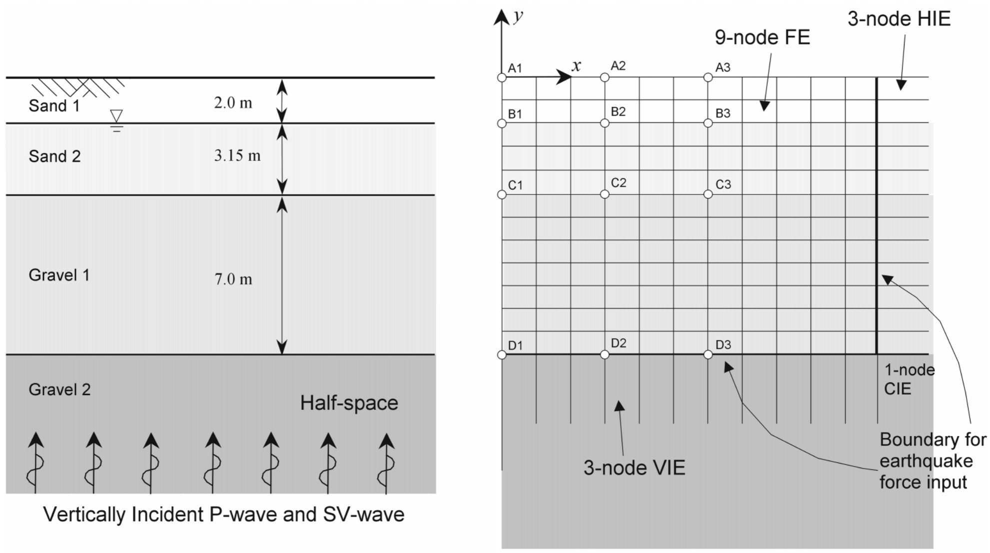

(a) Field field (b) Finite-infinite element mesh

Fig. 4 Earthquake response analysis of a layered soil medium

Table 2 Ground profile of a multi-layered half-space for free field analysis

Soil Layer \ Property	Layer Depth (m)	Mass Density (Mg/m^3)	Shear Wave Velocity (m/sec)	Poisson's Ratio
Sand 1	2.0	1.69	133	0.38
Sand 2	3.15	1.93	231	0.48
Gravel 1	7.0	2.42	333	0.47
Gravel 2 (Half-space)	∞	2.42	476	0.47

with plane strain finite elements and the remaining far field soil region is modeled by analytical frequency-dependent infinite elements. The properties of the soil layers are shown in Table 2. A horizontal acceleration record is used as the input control motion on the ground surface, which is the NS-component of an earthquake measured at Hualien, Taiwan on January 20, 1994. The peak ground acceleration is 0.0318 g, and the time history is shown in Fig. 5(a) (Ohsaki Research Institute 1994).

At first, the equivalent earthquake input force is computed along the interface (Γ_e) based on the free field responses obtained using the conventional method (Zhao and Valliappan 1993, Zhang and Zhao 1988). Then, by applying the calculated input forces, the earthquake responses are computed at several locations in the near field soil medium (A1-A3, B1-B3, C1-C3, and D1-D3 in Fig. 4) using the present earthquake response analysis method in the time domain. The acceleration histories are compared with those of the free field analysis which are obtained based on the frequency domain method. The results in Figs. 5 to 8 show excellent agreements. The response spectra of the responses are also compared in Fig. 9, which also shows very good agreements. In

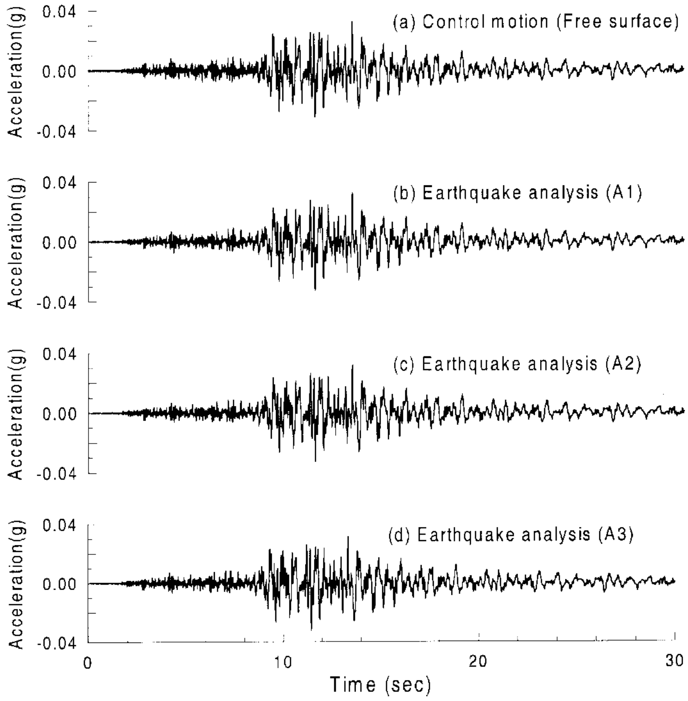

Fig. 5 Free-field and earthquake-response analysis results at surface

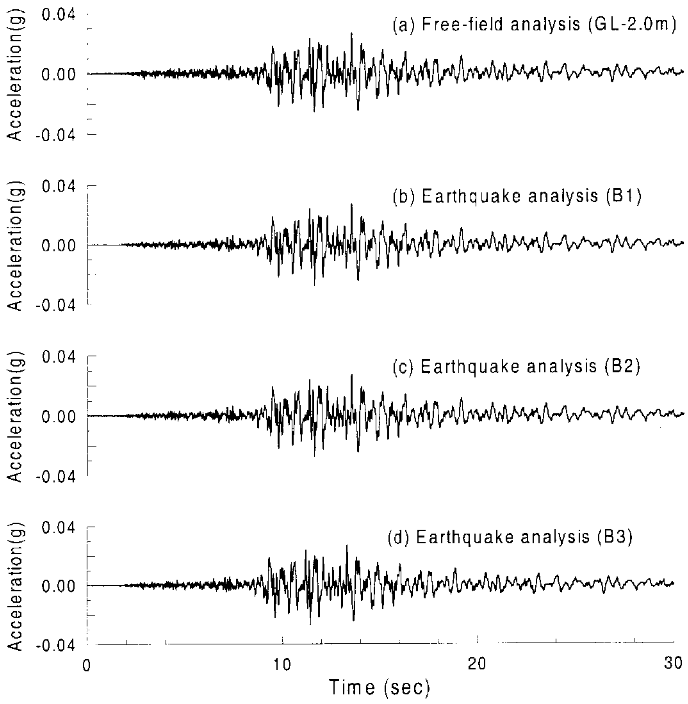

Fig. 6 Free-field and earthquake-response analysis results at GL-2.0 m

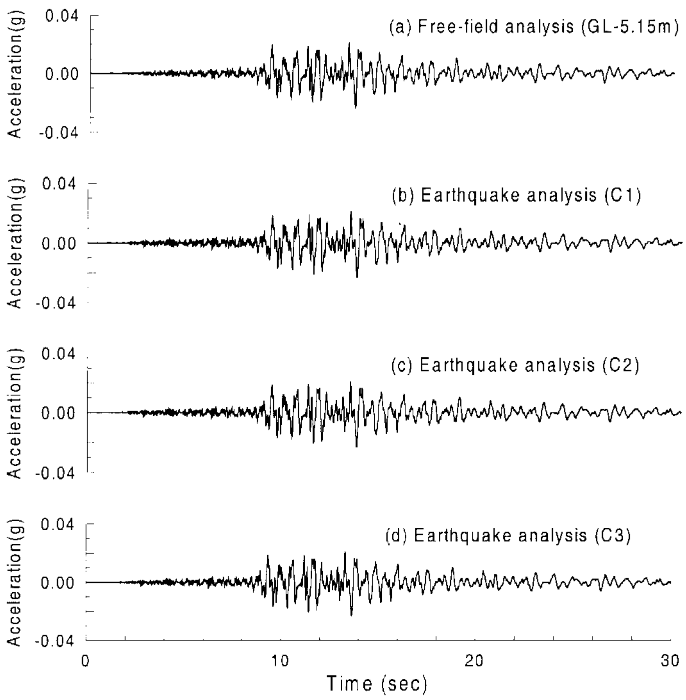

Fig. 7 Free-field and earthquake-response analysis results at GL-5.15 m

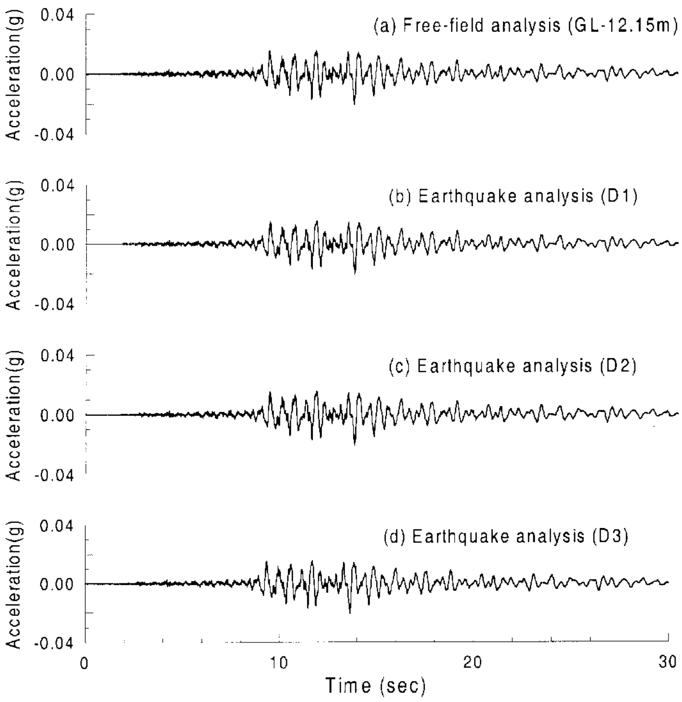

Fig. 8 Free-field and earthquake-response analysis results at GL-12.15 m

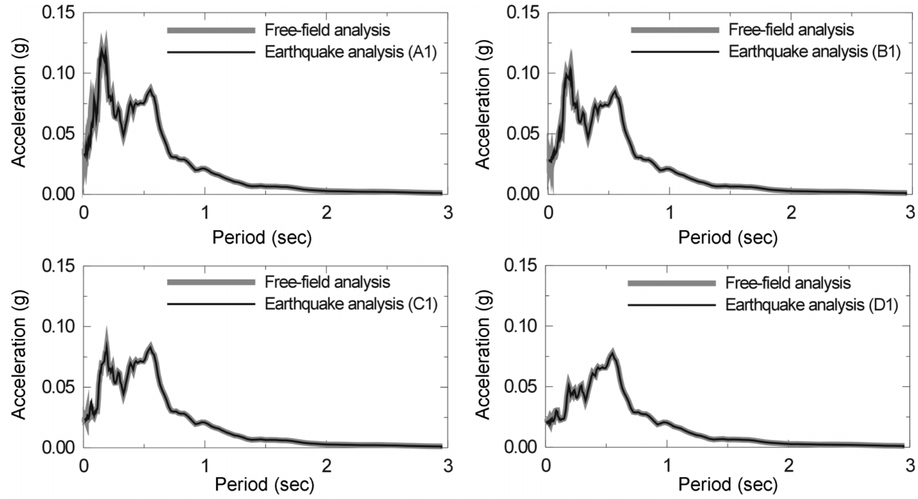

Fig. 9 Comparisons of response spectra

the present time domain formulation of Eq. (23), the mass, damping, and stiffness matrices of the total soil-structure interaction system are real-valued constants, because only the geometric damping of the unbounded soil medium is introduced excluding the material damping which is customarily expressed in complex form. However, the damping matrix may remain real-valued, if the material damping particularly in the near field region is approximated as equivalent viscous damping.

5.2 Response of a tunnel structure in a layered soil

Earthquake response analysis is also performed for a tunnel embedded in a layered half-space. A rectangular tunnel lining structure (Kim and Yun 2000, Estorff and Antes 1990) and the near field soil region are modeled by finite elements, while the far field soil region is represented by analytical frequency-dependent infinite elements as shown in Fig. 10. The dimension of the tunnel structure is taken as 5 m $\times$ 6 m, and the embedded depth is 4 m. The horizontal distance from the center of the tunnel to the HIE's is taken as 5*b* and the vertical depth from the ground surface to the VIE's is as 6*b*, where *b* is the half width of the tunnel. Two body wave components and two Rayleigh wave components are used in the infinite element formulation. For the tunnel structure, mass density (ρ_t) and Poisson's ratio (ν_t) are taken as 2 ton/m^3 and 0.25, and Young's modulus is 6 GPa. For the soil medium, material properties of a layered half-space are shown in Table 3. The same earthquake record used the previous example is taken as an input control motion on the ground surface.

The responses along several vertical profiles of the soil are compared with the free field responses in Fig. 11. It can be obtained that the horizontal response is affected by the soil-structure interaction, and the response approaches to those of the free field as the distance from the tunnel becomes far. In the present example, the duration of earthquakes is 40.96 sec with the step of 0.01 sec, and the total computational CPU time for the response of the tunnel structure in a layered soil was about 70 minutes by a personal computer with 1 GHz CPU, while 45 minutes for the free field responses in Section 5.1.

Table 3 Ground profile of a tunnel-soil system

Property / Soil Layer	Layer Depth (m)	Mass Density (Mg/m^3)	Shear Wave Velocity (m/sec)	Poisson's Ratio
Upper layer	12.0	2.0	250	0.40
Half-space	∞	2.0	500	0.40

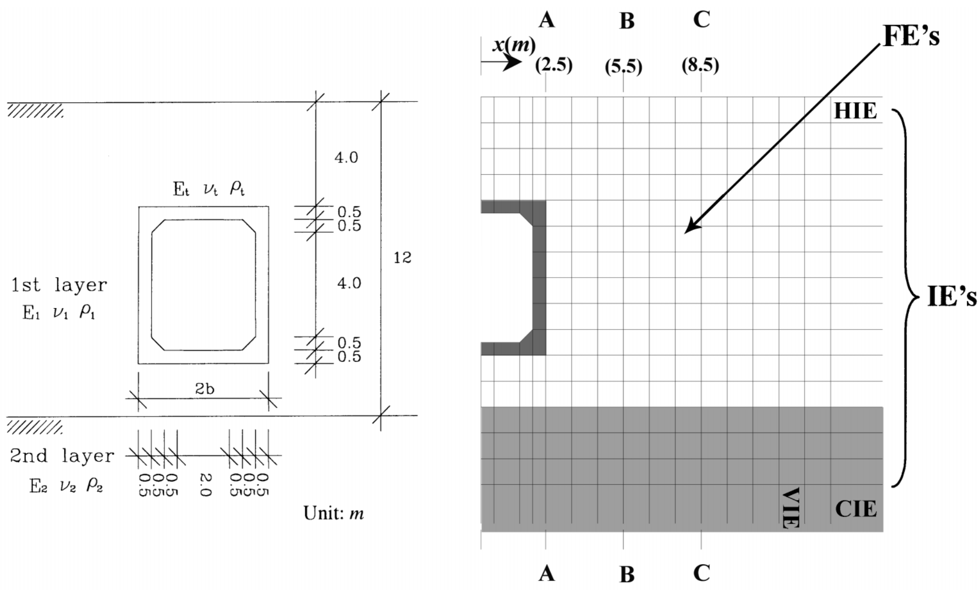

(a) Tunnel-soil interaction system (in *m*)   (b) Analysis model

Fig. 10 Tunnel in an layered half-space

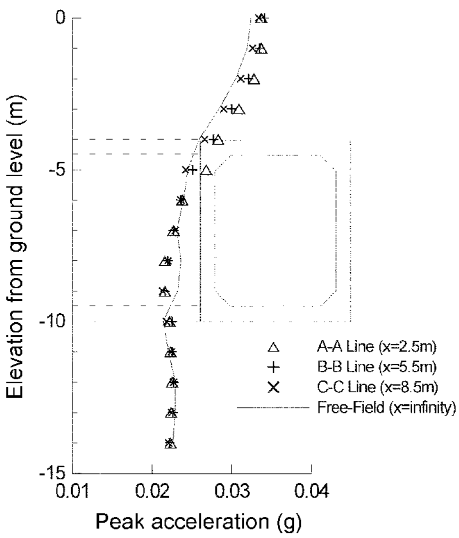

Fig. 11 Maximum horizontal acceleration of the soil medium

6. Conclusions

In this paper, an earthquake response analysis method in the time domain is developed and verified. For the modeling of a soil-structure interaction system, finite and analytical frequency-dependent infinite elements are adopted. For two dimensional earthquake response analyses, earthquake inputs are regarded as traveling P- and SV-waves that are incident vertically to the near field soil region. In which, the equivalent earthquake input forces in the frequency domain are calculated utilizing the fixed exterior boundary method and the free field responses. Then, the input forces are transformed into the time domain by using inverse Fourier transform. Earthquake response analyses of a multi-layered half-space have been carried out. The results are founded to be in good agreement with the free field responses obtained by the conventional frequency domain method. Earthquake response analysis has been also performed for a tunnel embedded in a layered half-space to show the applicability of the proposed method. It shows that the distribution of responses is affected by the soil-structure interaction, and the response approaches to the free field response as the distance from the tunnel becomes longer.

Acknowledgements

The authors are very grateful for the support from Smart Infra-Structure Technology Center sponsored by Ministry of Science and Technology and Korea Science and Engineering Foundation.

References

ASD International, Inc., CA. (1985), *CLASSI-ASD : Computer Program for 3-D/Multiple-Foundation Analysis*, Version 2.

Betti, R., Abdel-Grhaffar, A.M. and Niazy, A.S. (1993), "Kinematic soil-structure interaction for long-span cable-supported bridges", *Earth. Eng. Str. Dyn.*, **22**, 415-430.

Estorff, O.V. and Antes, H. (1990), "Dynamic response of tunnel structures", *Structural Dyn.*, Kratzig *et al.* (eds), 803-810.

Estorff, O.V. (1991), "Dynamic response of elastic blocks by time domain BEM and FEM", *Comp. Str.*, **38**(3), 289-300.

Guan, F. and Novak, M. (1994), "Transient response of an elastic homogeneous half-space to suddenly applied rectangular loading", *Transactions of the ASME*, **61**, 256-263.

Hayashi, Y. and Katukura, H. (1990), "Effective time-domain soil-structure interaction analysis based on FFT algorithm with casaulity condition", *Earth. Engrg. Str. Dyn.*, **19**, 693-708.

Karabalis, D.L. and Beskos, D.E. (1985), "Dynamic response of 3-D flexible foundations by time domain BEM and FEM", *Soil Dyn. Earthquake Eng.*, **4**, 91-101.

Kim, D.K. and Yun, C.B. (2000), "Time domain soil-structure interaction analysis in two dimensional medium based on analytical frequency-dependent infinite elements", *Int. J. Numer. Meth. Eng.*, **47**, 1241-1261.

Kramer, S.L. (1996), *Geotechnical Earthquake Engineering*, Prentice-Hall, Englewood Cliffs.

Lysmer, J., Udaka, T., Tsai, C.F. and Seed, H.B. (1975), "FLUSH - A computer program for approximate 3-D analysis of soil-structure interaction problems", *Report No. EERC 75-30*, Earthquake Engineering Research Center, University of California, Berkeley, CA.

Lysmer, J., Ostadan, F., Tabatabaie, H., Vahdani, S. and Tajirian, F. (1988), *SASSI–A System for Analysis of Soil-Structure Interaction*, Univ. of California, Berkeley, CA.

Ohsaki Research Institute (1994), "Blind prediction analysis of 1/20/94 earthquake", *Hualien LSST Meeting*, Palo Alto, CA, December.

Seed, H.B. and Idriss, I.M. (1970), "Soil moduli and damping factors for dynamic response analysis", *Report No. EERC 75-29*, Earthquake Engineering Research Center, University of California, Berkeley, CA.

Song, C. and Wolf, J.P. (1999), "The scaled boundary finite-element method–alias consistent infinitesimal finite-element cell method for elastodynamics", *Comput. Methods Appl. Mech. Eng.*, **147**(3-4), 329-355.

Tzong, T.J. and Penzien, J. (1983), "Hybrid modelling of soil-structure interaction in layered media", *Rep. No. UCB/EERC-83/22*, EERC, University of California, Berkeley, CA.

Wolf, J.P. (1985), *Dynamic Soil-Structure Interaction*, Prentice Hall.

Wolf, J.P. (1988), *Soil-Structure-Interaction Analysis in Time Domain*, Prentice Hall.

Wolf, J.P. and Song, C. (1996), *Finite-Element Modelling of Unbounded Media*, John Wiley & Sons.

Wolf, J.P. and Obernhuber, P. (1982), "Free field response from inclined SH-waves and Love-waves", *Earthq. Eng. Str. Dyn.*, **10**, 823-845.

Yun, C.B., Kim, D.K. and Kim, J.M. (2000), "Analytical frequency-dependent infinite elements for soil-structure interaction analysis in two-dimensional medium", *Engineering Structures*, **22**(3), 258-271.

Zhang, C. and Zhao, C. (1988), "Effects of canyon topography and geological condition on strong ground motion", *Earth. Eng. Str. Dyn.*, **16**, 81-97.

Zhang, X., Wegner, J.L. and Haddow, J.B. (1999), "Three-dimensional dynamic soil-structure interaction analysis in time domain", *Earth. Engrg. Str. Dyn.*, **28**(12), 1501-1524.

Zhao, C. and Valliappan, S. (1993), "An efficient wave input procedure for infinite media", *Communications in Numerical Methods in Engineering*, **9**, 407-415.